Editorial Manager(tm) for Journal of Geodesy
Manuscript Draft

Manuscript Number:

Title: Rapid re-convergences to ambiguity-fixed solutions in precise point positioning

Article Type: Original Article

Keywords: precise point positioning; ambiguity resolution; rapid re-convergence; predicted ionospheric delays

Corresponding Author: Mr. Jianghui Geng, MSc

Corresponding Author's Institution: Institute of Engineering Surveying and Space Geodesy

First Author: Jianghui Geng, MSc

Order of Authors: Jianghui Geng, MSc; Xiaolin Meng, PhD; Alan H Dodson, PhD; Maorong Ge, PhD; Felix N Teferle, PhD

Abstract: Integer ambiguity resolution at a single station can be preformed if the fractional-cycle biases are separated from the ambiguity estimates in precise point positioning (PPP). Despite the improved positioning accuracy by such integer resolutions, the convergence to an ambiguity-fixed solution normally requires at least a few tens of minutes. More importantly, such convergences can repeatedly occur on the occasion of losses of tracking locks for many satellites if an open sky-view is not constantly available, consequently totally destroying the practicability of real-time PPP. In this study, in case of such re-convergences, we develop a method in which ionospheric delays are precisely predicted to significantly accelerate integer ambiguity resolutions. The effectiveness of this method consists in two aspects: First, wide-lane ambiguities can be rapidly resolved using the ionosphere-corrected wide-lane measurements, instead of the noisy Melbourne-Wübbena combination measurements; second, narrow-lane ambiguity resolution can be accelerated under the tight constraints derived from the ionosphere-corrected unambiguous wide-lane measurements. In the tests at 90 static stations suffering from simulated total loss of tracking locks, 93.3% and 95.0% of re-convergences to wide-lane and narrow-lane ambiguity resolutions can be achieved within 5 s, respectively, even though the time latency for the predicted ionospheric delays is up to 180 s. In the tests at a mobile van moving in a GPS-adverse environment where satellite number significantly decreases and cycle slips frequently occur, only when the predicted ionospheric delays are applied can the rate of ambiguity-fixed epochs be dramatically improved from 7.7% to 93.6% of all epochs. Therefore, this method can potentially relieve the unrealistic requirement of a continuous open sky-view by most PPP applications and improve the practicability of real-time PPP.

Suggested Reviewers: Yan Kouba PhD
Geodetic Survey Division, Natural Resources Canada
kouba@geod.nrcan.gc.ca
Dr Kouba is an expert in PPP technology development.

Flavien Mercier PhD
Centre National d'Etudes Spatiales, France
flavien.mercier@cnes.fr

Dr Mercier developed a method for PPP ambiguity resolution, and he is interested in rapid ambiguity resolution.

Rapid re-convergences to ambiguity-fixed solutions in precise point positioning

[1]Jianghui Geng, [1]Xiaolin Meng, [1]Alan H Dodson, [2]Maorong Ge, [3]Felix N Teferle

[1]*Institute of Engineering Surveying and Space Geodesy, University of Nottingham, NG7 2TU, UK*
[2]*GeoForschungsZentrum Helmholtz Center, Potsdam, 14473, Germany*
[3]*Faculty of Science, Technology and Communication, University of Luxemburg, L-1359, Luxemburg*

Abstract: Integer ambiguity resolution at a single station can be preformed if the fractional-cycle biases are separated from the ambiguity estimates in precise point positioning (PPP). Despite the improved positioning accuracy by such integer resolutions, the convergence to an ambiguity-fixed solution normally requires at least a few tens of minutes. More importantly, such convergences can repeatedly occur on the occasion of losses of tracking locks for many satellites if an open sky-view is not constantly available, consequently totally destroying the practicability of real-time PPP. In this study, in case of such re-convergences, we develop a method in which ionospheric delays are precisely predicted to significantly accelerate integer ambiguity resolutions. The effectiveness of this method consists in two aspects: First, wide-lane ambiguities can be rapidly resolved using the ionosphere-corrected wide-lane measurements, instead of the noisy Melbourne-Wübbena combination measurements; second, narrow-lane ambiguity resolution can be accelerated under the tight constraints derived from the ionosphere-corrected unambiguous wide-lane measurements. In the tests at 90 static stations suffering from simulated total loss of tracking locks, 93.3% and 95.0% of re-convergences to wide-lane and narrow-lane ambiguity resolutions can be achieved within 5 s, respectively, even though the time latency for the predicted ionospheric delays is up to 180 s. In the tests at a mobile van moving in a GPS-adverse environment where satellite number significantly decreases and cycle slips frequently occur, only when the predicted ionospheric delays are applied can the rate of ambiguity-fixed epochs be dramatically improved from 7.7% to 93.6% of all epochs. Therefore, this method can potentially relieve the unrealistic requirement of a continuous open sky-view by most PPP applications and improve the practicability of real-time PPP.
Keywords: precise point positioning; ambiguity resolution; rapid re-convergence; predicted ionospheric delays

1 Introduction

Double-difference carrier-phase ambiguities can normally be fixed to integers in precise GPS (Global Positioning System) applications. Nonetheless, undifferenced ambiguities in precise point positioning (PPP) (Zumberge et al. 1997) lose the integer properties because they absorb the fractional-cycle biases (FCBs) that originate from both receiver and satellite hardware. Fortunately, the integer properties can be retrieved by correcting the FCBs estimated using a network of reference stations (e.g. Ge et al. 2008). Due to the ionosphere-free observable used in PPP, integer ambiguity resolution is performed through two sequential steps: Wide-lane ambiguities are first resolved using the Melbourne-Wübbena combination observable (Melbourne 1985; Wübbena 1985); and narrow-lane ambiguities are then resolved based on the resulting integer wide-lane ambiguities (Collins 2008; Geng et al. 2009; Laurichesse et al. 2009). Geng et al. (2010) illustrated that integer ambiguity resolution can significantly improve the positioning accuracy from decimeter to centimeter level in real-time PPP.

Nevertheless, a long convergence period to such an ambiguity-fixed solution considerably devaluates the accuracy improvement contributed by integer resolutions. In terms of a substantial data processing, Geng

et al. (2010) concluded that at least 10 minutes are required to resolve about 90% of wide-lane ambiguities, whereas over 10 minutes for a narrow-lane ambiguity resolution. A wide-lane ambiguity is estimated based on the noisy Melbourne-Wübbena combination measurements, and thus a long period is required to sufficiently smooth the noise. On the other hand, a long period for the narrow-lane resolution is largely attributed to the imprecise pseudorange measurements which cannot sufficiently shrink the search space for integer ambiguities suffering from a rather short wavelength of 10.7 cm (Teunissen 1996). Hence, a long observation period has to be used to average out sufficiently precise pseudoragne measurements before deriving accurate ambiguity estimates (Teunissen et al. 1997). To date, however, it is still extremely hard to develop an effective method to accelerate such convergences.

More importantly, such convergences of long period can repeatedly occur on the occasion of losses of tracking locks for many satellites. As usual events in industrial applications, frequent re-convergences can totally destroy the practicability of real-time PPP. As a result, a continuous open sky-view is constantly required by most PPP applications to maintain a centimeter-level positioning accuracy (Bisnath and Gao 2007). To relieve this unrealistic requirement and improve the practicability of PPP, Banville and Langley (2009) identified the integer cycle slips caused by such lock losses through differencing between epochs, simply assuming that ionospheric delays canceled out during such differences. However, they did not perform integer resolutions on undifferenced ambiguities. On the other hand, Geng (2009) developed a method where ionospheric delays were precisely predicted to tightly constrain the narrow-lane resolutions to significantly accelerate re-convergences. Encouragingly, the re-convergence periods were shortened from about 1000 to 20 s on average with a success rate of around 90%. Nevertheless, Melbourne-Wübbena combination measurements were still used to fix wide-lane ambiguities, thereby hardly guaranteeing a rapid re-convergence of only a few seconds.

In this study, we aim at improving this method to achieve rapid re-convergences to ambiguity-fixed solutions within a few seconds. Note that "convergence" throughout this study implies "achieving ambiguity-fixed solutions". In the following, Section 2 details the theories of this method; Section 3 presents a case study at static stations, investigates the impacts of time latency on the prediction error of ionospheric delays and discusses the efficiency of rapid re-convergences; Section 4 presents a case study at a mobile van, investigates the performance of rapid re-convergences in a GPS-adverse environment where satellite number significantly decreases and cycle slips frequently occur, and compares the results with the network real-time kinematic (NRTK) solutions; finally, Section 5 summarizes the main points and addresses the perspective of a wide-area PPP-RTK service supported by rapid ambiguity resolution.

2 Method

In terms of the previous section, the keys to accelerating convergences consist in both avoiding the Melbourne-Wübbena combination measurements and shrinking the search space for integer ambiguities. The volume of this search space is governed by the variance-covariance matrix of ambiguity estimates, and it approximately observes the following rule (Teunissen 1996 and 1997):

$$V \propto \frac{\sigma_p}{n\lambda} \tag{1}$$

where V is the volume of search space; σ_p is the precision of pseudorange or unambiguous measurements; n is the number of epochs; λ is the wavelength of carrier-phase measurements; and $\propto$ denotes a proportional relationship. To achieve rapid convergences, increasing n is unrealistic, and thus

we can only diminish σ_p and enlarge λ. In this section, we thereby derive how to precisely predict ionospheric delays and how to apply these delays to accelerate both the wide-lane and narrow-lane ambiguity resolutions, and then discuss the implementation of this method.

2.1 Precisely predict ionospheric delays

In general, GPS carrier-phase measurements on frequency g $(g=1,2)$ at a particular epoch for a single receiver can be written as

$$\lambda_g \Phi_g^s = \rho^s + ct - ct^s + T^s - \frac{\kappa^s}{f_g^2} + \lambda_g \left(B_g + B_g^s + N_g^s \right) + \varepsilon_g^s \tag{2}$$

where the superscript s $(s=1,\cdots)$ denotes a satellite s; Φ_g^s is the carrier-phase measurement where antenna phase center corrections have been applied; λ_g is the wavelength and f_g is the frequency; c is the light speed; ρ^s is the geometric distance between the receiver and the satellite s; t and t^s are the receiver and satellite clock errors, respectively; T^s denotes a slant tropospheric delay; $\frac{\kappa^s}{f_g^2}$ denotes a slant ionospheric delay; N_g^s denotes an integer ambiguity; B_g and B_g^s are the receiver and satellite FCBs, respectively; finally, ε_g^s denotes unmodeled errors including multipath effects. From Equation 2, a wide-lane measurement can be formed as

$$\lambda_w \Phi_w^s = \frac{\kappa^s}{f_1 f_2} + \rho^s + ct - ct^s + T^s + \lambda_w \left(B_w + B_w^s + N_w^s \right) + \varepsilon_w^s \tag{3}$$

where λ_w is the wide-lane wavelength of about 86 cm; $\Phi_w^s = \Phi_1^s - \Phi_2^s$, $B_w = B_1 - B_2$, $B_w^s = B_1^s - B_2^s$, $N_w^s = N_1^s - N_2^s$ and $\varepsilon_w^s = \varepsilon_1^s - \varepsilon_2^s$. In this study, Equation 3 is hereafter used to estimate the ionospheric delay, namely the term of $\frac{\kappa^s}{f_1 f_2}$ in theory. For a low-dynamic receiver, the ionospheric delays corresponding to each satellite manifest a strong temporal correlation over a few minutes (Dai et al. 2003; Kashani et al. 2007).

Despite this favorable characteristic of ionospheric delays, we further have to quantify the residual biases possibly assimilated into the estimate of $\frac{\kappa^s}{f_1 f_2}$ and investigate the temporal characteristics of these biases. First, the receiver clock error seems an unstable quantity over time. Hence, a single difference between satellites j and k can be formed to eliminate the receiver clocks, namely

$$\lambda_w \Phi_w^{jk} = \frac{\kappa^{jk}}{f_1 f_2} + \lambda_w \left(B_w^{jk} + N_w^{jk} \right) + \rho^{jk} - ct^{jk} + T^{jk} + \varepsilon_w^{jk} \tag{4}$$

Note that the receiver FCB is also removed. The satellite FCB B_w^{jk} is normally deemed rather stable over at least 24 hours (Ge et al. 2008; Laurichesse et al. 2009), and the integer N_w^{jk} is derived from the previous ambiguity-fixed solution.

Second, ρ^{jk} depends on both the receiver and satellite positions. To date, predicted GPS satellite orbits over 24 hours have reached an accuracy of around 5 cm (http://igscb.jpl.nasa.gov/components/prods.html). Residual radial orbit errors can be mostly mitigated by satellite clocks (Senior et al. 2008), if a consistent yaw-attitude model is applied to GPS satellites (Kouba 2009). Moreover, GPS satellite orbits are tightly constrained by dynamic force models, and thus the residual orbit errors should change smoothly in theory. On the other hand, for a re-convergence, the receiver position can be known to the centimeter-level accuracy from previous ambiguity-fixed solutions (Geng et al. 2010).

Third, due to the high correlation between t^{jk} and the satellite orbits (Senior et al. 2008), favorable user range errors of centimeter level can be achieved (Hauschild and Montenbruck 2009). Nonetheless, this t^{jk} is normally a predicted value due to the communication delays in real-time applications. Fortunately, Senior et al. (2008) reported that the Rubidium and Cesium clocks on current GPS satellites can be precisely predicted to a precision of better than 0.1 ns up to a period of 40 s which covers typical communication delays.

Fourth, T^{jk} can be mostly mitigated by estimating a zenith tropospheric delay (ZTD) based on a mapping function. Residual tropospheric delays are only a few millimeters at high elevations, but can be up to several centimeters at an elevation of smaller than 10° (Stoew et al. 2007). However, the troposphere condition around a low-dynamic receiver normally changes very slightly over at least several minutes if no pronounced height variation occurs for this receiver (Dai et al. 2003; Shan et al. 2007). Considering this similar temporal property to that of ionospheric delays, we can alternatively combine the two atmospheric delays and predict their sum over time.

Finally, ε_w^{jk} is the most uncertain quantity in Equation 4 and we believe that the multipath effect dominates among all possible unmodeled errors. Dilßner et al. (2008) showed that the carrier-phase biases caused by multipath effects stemming from solely radiating near fields can theoretically reach a few centimeters for low-elevation satellites. Although Han and Rizos (2000) described the strong temporal correlation of the multipath signatures at static antennas, the signatures can be quite random and thus unpredictable at mobile antennas.

Knowing the quantities of N_w^{jk}, ρ^{jk}, t^{jk} and T^{jk}, we can deduct them from Φ_w^{jk} in terms of Equation 4 and estimate the ionospheric delay

$$I_w^{jk} = \frac{\kappa^{jk}}{f_1 f_2} + \lambda_w B_w^{jk} + e_w^{jk} + \varepsilon_w^{jk} \tag{5}$$

where e_w^{jk} contains the errors caused by the receiver position, the satellite products and the tropospheric delays. In terms of the quantitative assessments above, we can infer that $e_w^{jk} + \varepsilon_w^{jk}$ can easily amount to over 10 cm for low-elevation satellites. Fortunately, B_w^{jk} changes negligibly over a long time and e_w^{jk} changes slightly or predictably over a few minutes, thereby minimally affecting the temporal-correlation characteristic of $\frac{\kappa^{jk}}{f_1 f_2}$. Hence, I_w^{jk} can be precisely predicted over at least a few minutes, especially at

static stations where multipath effects are also temporally correlated. In this study, I_w^{jk} is called "ionospheric delay" for brevity although it contains more than an ionospheric delay.

For the predicting strategy, we suggest the linear fitting model where estimated ionospheric delays within a sliding time window are used to fit a linear function, and a predicted delay is then computed using this function (Dai et al. 2003). In this study, the time span between a predicted and the latest estimated ionospheric delay is named as the latency of this predicted delay. This time latency can be caused by data gaps, for example. The prediction error is quantified by differencing the predicted and estimated ionospheric delays at a particular epoch. Geng (2009) illustrated that the prediction error is increased when the elevation angle is smaller and the time latency is longer, and this increasing rate depends on the ionosphere condition. Hence, besides the elevation-dependent weighting by Geng (2009), a latency-dependent weighting on the predicted ionospheric delays is also required, such as

$$p\left(t_l\right)=\begin{cases}1.0 & t_l < 30.0 \text{ s} \\ \tan\left(\dfrac{\pi}{4}\cdot\dfrac{30.0}{t_l}\right) & t_l \geq 30.0 \text{ s}\end{cases} \tag{6}$$

where t_l is the time latency in seconds and the "30 s" will be illustrated in Section 3.2.

2.2 Rapidly retrieve integer ambiguities

Integer ambiguities can be rapidly retrieved by applying the precisely predicted ionospheric delays after a re-convergence occurs. This is achieved by two steps. First, wide-lane measurements are formed using Equation 4 and are corrected by the known satellite products, the latest ZTD estimate, and the predicted ionospheric delays. If the time latency is smaller than a few minutes, the errors caused by FCBs, satellite products and atmospheric delays can be canceled out or mostly mitigated by the counterparts in the predicted ionospheric delays (Dai et al. 2003; Kashani et al. 2007). Note that unmodeled errors are not easy to predict and are thereby supposed to be sufficiently small in this study. Finally, we obtain

$$\lambda_w \Phi_w^{jk} = \rho^{jk} + \lambda_w N_w^{jk} + \zeta_w^{jk} \tag{7}$$

where ζ_w^{jk} contains the unmodeled errors and the prediction error of ionospheric delays, and it actually quantifies the precision of Equation 7; only the positions and ambiguities are unknown. Aided by the ionosphere-free pseudorange measurements, the wide-lane ambiguity N_w^{jk} can be resolved using Equation 7 if ζ_w^{jk} is small enough (e.g. $<1/4\,\lambda_w$). In terms of Equation 1, thanks to the relatively long wavelength for wide-lane ambiguities, ionosphere-free pseudorange measurements can normally sufficiently shrink the search space to only a few integer candidates (Teunissen 1996 and 1997), thereby improving the search efficiency and accelerating the identification of integer ambiguities.

Second, once the wide-lane ambiguity is successfully resolved, Equation 7 becomes a precise unambiguous measurement, namely

$$\lambda_w \Phi_w^{jk} - \lambda_w N_w^{jk} = \rho^{jk} + \zeta_w^{jk} \tag{8}$$

Equation 8, rather than the pseudorange measurements, can be used to constrain the integer identification of narrow-lane ambiguities. In terms of Equation 1, if the magnitude of ζ_w^{jk} is far smaller than a few centimeters, applying Equation 8 can considerably shrink the search space for narrow-lane ambiguities to a few integer candidates (Teunissen 1996 and 1997). As a result, narrow-lane ambiguity resolution can be

accelerated. Note that the prediction error of ionospheric delays dominates ζ_w^{jk} if the time latency is long. An imprecisely predicted ionospheric delay will weaken the constraint by Equation 8, possibly failing a rapid re-convergence.

Finally, we stress that both rapid resolutions above do not rely on satellite geometry changes, but the sufficient shrink of search space for integer candidates. Such shrinks are achieved by applying the ionosphere-free pseudorange and the ionosphere-corrected unambiguous wide-lane measurements which are precise enough relative to the wide-lane and narrow-lane wavelengths, respectively. Hence, float ambiguity estimates are close to correct integers and these integers can then be relatively easily identified, even though only a few epochs of measurements are used.

2.3 Remarks on the method implementation

From the method description above, the prerequisite of this method is how to precisely predict ionospheric delays, which depends on three aspects:

- Temporal properties of all errors in the ionospheric delay by Equation 5. Although the true ionospheric delay dominates its temporal variation, other errors including clock predictions and multipath effects should also be carefully regarded;
- Predicting strategy. Currently, it is not easy to precisely predict the ionosphere condition over a long time due to its complicated relationships with the geomagnetic field, the solar activity etc. especially during an ionospheric storm. Temporal ionospheric irregularities cannot be precisely depicted beforehand in real-time applications. In this case, only the linear trend of the ionosphere change can usually be depicted with a relatively high confidence level (Dai et al. 2003);
- Model consistence between the ionospheric delay estimation using Equation 5 and the wide-lane ambiguity resolution using Equation 7. Note that both models are derived from Equation 4. In this manner, their common biases can naturally cancel out without impairing the integer ambiguities, hence explaining why we do not care about the accuracy of the estimated ionospheric delays.

Heretofore, we need to acknowledge that this method applies to only rapid re-convergences because ionospheric delays have to be generated at a precisely known position. Nonetheless, if a dense network of reference stations is available, ionospheric delays can also be estimated at the reference stations and then interpolated at single users to assist rapid convergences. In this case, the first ambiguity-fixed solutions can also be achieved rapidly.

In this study, we implement this method mainly for rapid re-convergences, but rapid convergences by a dense network are also discussed. For integer resolutions, we used the least-squares ambiguity decorrelation adjustment method (Teunissen 1996) to search for integer candidates. All available satellites over an elevation angle of 7° were used for wide-lane ambiguity resolution, whereas those over 15° for narrow-lane ambiguity resolution. For the clock determination and the FCB determination, we refer to Geng (2009) and Geng et al. (2010). Note that communication delays were ignored in our simulated real-time study. In the following, we will detail two case studies at static and mobile receivers to assess this method. The improved PANDA (Positioning and Navigation Data Analyst) software (Shi et al. 2008) was used for this study.

3 A case study at static stations

In this section, we investigate the prediction error of ionospheric delays, and assess this method at static stations by quantifying the success rate and the time to ambiguity-fixed solutions.

3.1 Data processing

Seven days of 24-hour 1-Hz GPS data from July 6th to 12th in 2008 at about 90 stations across Europe were collected from the European Reference Frame – Internet Protocol project and the Ordnance Survey of Great Britain real-time network (Figure 1). Of particular note, these data bear the gaps caused by communication and power interruptions etc. The Kp index, which quantifies the ionosphere activity level, was below 4 on average during these days, thus showing a moderate ionosphere condition. At these stations, positions were estimated as white noise at each epoch, and ZTDs were estimated every three hours. In order to test rapid re-convergences, we introduced a total signal interruption 20 minutes after each successful convergence, and thus each station suffered from about 70 re-convergences per day if there were no large data gaps. For each re-convergence, we set a time latency for the predicted ionospheric delays to simulate a data gap. We believe that this data set is quite representative because it covers 24 hours per day and contains stations working in different environments.

3.2 Prediction error of ionospheric delays

The prediction error of ionospheric delays is subject to both the time latency and the elevation angle. In Figure 2, the ionospheric delays at a typical station ACOR are divided into two groups using an elevation angle of 30°. The RMS of their prediction errors for all satellite pairs during 24 hours is plotted against both the time latency and the time window width for the linear fitting model. As expected, the RMS is increased when the time latency is prolonged. However, enlarging the window width can slow down this increasing rate. As a large window width degrades the computation efficiency, we finally choose 120 s as a trade-off for the ionospheric delays above 30° whereas 240 s for those below 30° in this study. It can be seen that the error for a 300-second prediction is only 3.7 cm for the ionospheric delays over 30° and 7.3 cm for those below 30°. Additionally, the prediction error remains steady when the time latency is smaller than 30 s, explaining why equal weights are posed within 30 s in Equation 6.

3.3 Performance of rapid re-convergences

Applying the precisely predicted ionospheric delays can significantly improve the success rate of rapid re-convergences and shorten the time spent on these re-convergences. Table 1 shows the statistics about the rapid re-convergences achieved within 5 s under different time latencies. When the time latency is 10 s, 99.4% and 98.7% of re-convergences to wide-lane and narrow-lane ambiguity resolutions can be rapidly achieved, respectively. Even though the time latency is up to 180 s, these two percentages can still reach 93.3% and 95.0%. For comparison, if we do not apply this method, only 78.9% of all re-convergences can be achieved within 20 minutes with a mean time of 694 s. However, when the time latency is up to 300 s, the above two percentages steadily fall to 85.8% and 77.5%. This deterioration can be understood in terms of the amplified prediction error of ionospheric delays. From Equation 7, ionospheric delays of large prediction errors will enlarge the magnitude of ζ_w^{jk}, hence possibly biasing the corresponding wide-lane ambiguity estimates and degrading the reliability of integer resolutions. Furthermore, even though a rapid wide-lane ambiguity resolution can be achieved, a large ζ_w^{jk} will lead to a poor precision of an unambiguous measurement by Equation 8, hence weakening the resulting constraint on the subsequent narrow-lane ambiguity resolution. Additionally, when the time latency is only 10 s, the failure rates for

the wide-lane and narrow-lane resolutions account for 0.6% and 1.3%, respectively, most of which are caused by low satellite availability and poor satellite geometry.

On the other hand, Table 1 also presents the mean times to fix wide-lane and narrow-lane ambiguities. Note that the time to fix a narrow-lane ambiguity begins after a successful wide-lane ambiguity resolution. When the time latency is 10 s, approximately only 1 s of data is required to resolve wide-lane ambiguities, whereas almost no more time is required to resolve narrow-lane ambiguities. Overall, increasing the time latency will lead to longer times spent on achieving ambiguity-fixed solutions. However, these times are increased moderately or even minimally, implying that most rapid re-convergences are achieved within 1 s, even though the time latency is up to 300 s. In fact, this finding verifies that the satellite geometry change minimally contributes to the rapid re-convergences in this study.

4 A case study at a mobile van

In this section, we assess this method at a van moving in a GPS-adverse environment, then interpolate ionospheric delays based on a dense reference network and finally compare the results with those from a commercial NRTK service.

4.1 Data processing

A van-borne 1-Hz GPS data set was collected in the city of Nottingham on May 11th in 2009, covering about 2.5 hours from 11:30 to 14:04 (Local time). The Kp index was around 1 during this period, showing a quiet ionosphere condition. As shown in Figure 3, the van stopped or moved in four phases: 1) it stopped from 11:40 to 12:27 on a car park with an open sky view; 2) it moved from 12:27 to 13:12 along the red routes escorted by tall buildings, large trucks and thick trees; 3) it stopped again from 13:12 to 13:44 on the car park; 4) finally, it moved again from 13:44 to 14:04 along the blue routes on the car park with a few thick trees around. A reference station was located on top of the IESSG building which was within 2 km from the van. Moreover, this reference station was surrounded by other six reference stations within a distance from about 50 to 100 km. They were used to interpolate ionospheric and tropospheric delays. Additionally, the lower inset shows the satellite number which kept steady during the stopping phases, but changed dramatically during the moving phases due to signal obstructions.

At this van, we applied the phase wind-up corrections, although the antenna attitudes during the moving phases were unknown (Kim et al. 2006). No antenna phase center corrections were applied. We estimated only one ZTD during this experiment because the time span was short and the area was small. A ground truth was computed using the Leica Geo Office software of version 3.0 and the IESSG station is used as reference. We believe that the 3D accuracy of this ground truth should be better than a few centimeters. Moreover, an NRTK solution provided by the Leica SmartNet service was also collected for comparison.

4.2 Rapid convergences in a GPS-adverse environment

In a GPS-adverse environment, frequent and severe signal obstructions can significantly jeopardize the positioning performance and the ambiguity resolution. In Figure 4, for the ambiguity-float solutions, a clear trend is present for the East component and a bias is present for the North component. During the second phase when signals are frequently obstructed, all three components, especially vertical, experience large position errors of over a few decimeters. If the ambiguities are resolved, the positioning accuracy can be clearly improved for all three components, but this improvement only appears during the stopping

phases as shown in Figure 4. Ambiguity-fixed solutions were quickly and totally lost after the moving phases began. This is because re-convergences occurred due to the signal obstructions. Overall, the rate of ambiguity-fixed epochs is only 7.7% of all epochs during the moving phases.

Nevertheless, by further applying the method for rapid re-convergences, ambiguity-fixed solutions can be well maintained during the moving phases. From Figure 4, the accuracies of both horizontal components are better than 5 cm, whereas that of vertical is better than 10 cm during all four phases. Large position errors are present at only a few epochs when ambiguity-fixed solutions cannot be achieved. More importantly, the rate of ambiguity-fixed epochs is significantly increased up to 93.6% of all epochs during the moving phases, showing a significant improvement over the ambiguity-fixed solutions without rapid re-convergences. However, the first ambiguity-fixed solution is achieved after a few tens of minutes. To overcome this defect, the six surrounding reference stations are used to interpolate the ionospheric delays at this van. As a result, only 5 s of measurements are used to achieve the first ambiguity-fixed solution and the epochs with large position errors become much fewer, as shown in Figure 4. In fact, the rate of ambiguity-fixed epochs reaches up to 97.2% of all epochs during the moving phases. This improvement is largely attributed to the interpolated ionospheric delays which are more reliable than the predicted ones.

4.3 Comparisons with NRTK solutions

Normally, a NRTK service can generate centimeter-level positioning accuracy using double-difference measurements based on an RTK network. At the bottom of Figure 4, we present the position differences of a NRTK solution against the ground truth. Note that the gaps are caused by the unavailability of NRTK solutions. Large positioning errors occur from 13:40 to 13:50, and thus are excluded from the following statistics. It can be clearly seen that biases are present in all three components. We believe that these biases are largely caused by the strategies of applying antenna phase center corrections. Disregarding these discrepancies, we find that the ambiguity-fixed solutions aided by the ionospheric delays perform comparably with the NRTK solutions. In detail, the standard deviations of the differences for the East, North and Up components during the moving phases are 1.0, 1.3 and 2.7 cm for the ambiguity-fixed solutions with rapid re-convergences, respectively, whereas 0.6, 1.0 and 1.4 cm for the NRTK solutions. Of particular note, although comparable, the absolute position differences for the NRTK solutions are clearly smaller than those of the ambiguity-fixed solutions aided by ionospheric delays during the moving phases. We believe that this issue is mainly because the phase wind-up corrections cannot be precisely modeled as the antenna attitudes are unknown during the moving phases (Kim et al. 2006).

5 Conclusions and perspective

In this study, we develop a method where the ionospheric delays are predicted to the succeeding epochs to accelerate the ambiguity resolution in case of re-convergences. In theory, the effectiveness of this method consists in two aspects: On the one hand, wide-lane ambiguities can be rapidly resolved using the ionosphere-corrected wide-lane measurements, instead of the noisy Melbourne-Wübbena combination measurements; on the other hand, narrow-lane ambiguities can be rapidly resolved under the tight constraints derived from ionosphere-corrected unambiguous wide-lane measurements.

This method is verified by two tests. At static stations suffering from simulated losses of tracking locks for all satellites, even if the time latency for the predicted ionospheric delays is up to 180 s, 93.3% and 95.0% of re-convergences to wide-lane and narrow-lane ambiguity resolutions can be achieved within 5 s,

respectively. If this time latency is prolonged, the prediction error of ionospheric delays is increased, hence reducing both percentages above. On the other hand, most times spent on achieving ambiguity-fixed solutions are within 1 s, implying that the contribution of satellite geometry changes to these rapid re-convergences is minimal. At a mobile van moving in a GPS-adverse environment, ambiguity-fixed solutions can be well maintained when rapid re-convergences are achieved. The rate of ambiguity-fixed epochs is significantly improved from 7.7% to 93.6% of all epochs. Additionally, the RMS of position differences against the ground truth are 1.0, 1.3 and 2.7 cm for the East, North and Up components, respectively, which are comparable with those of the NRTK solutions.

Finally, the ionospheric delays can also be interpolated from a dense network of reference stations. Although such networks are normally not available for PPP, we can envision that if precise ionospheric delays can be derived from a sparse network at scales of several hundred kilometers using an ionospheric tomography technique (e.g. Hernández-Pajares et al. 2000), a PPP-RTK service (Geng et al. 2010) that can rapidly provide ambiguity-fixed solutions may potentially prevail against current RTK positioning services based on dense networks.

Acknowledgements

The authors thank the IGS community, the EUREF – Internet Protocol project and the Ordnance Survey of Great Britain for the data provision. Thanks also go to Wuhan University in China for the provision of PANDA software as collaborative research and development.

References

Banville S, Langley RB (2009) Improving real-time kinematic PPP with instantaneous cycle-slip correction. In: Proceedings of ION GNSS 22nd International Technical Meeting of the Satellite Division, Savannah, US, pp 2470-2478

Bisnath S, Gao Y (2007) Current state of precise point positioning and future prospects and limitations. In: Sideris MG (Ed) Observing our changing Earth, Springer-Verlag, New York, pp 615-623

Collins P (2008) Isolating and estimating undifferenced GPS integer ambiguities. In: Proceedings of ION National Technical Meeting, San Diego, US, pp 720-732

Dai L, Wang J, Rizos C, Han S (2003) Predicting atmospheric biases for real-time ambiguity resolution in GPS/GLONASS reference station networks. J Geod 76(11-12):617-628

Dilßner F, Seeber G, Wübbena G, Schmitz M (2008) Impact of near-field effects on the GNSS position solution. In: Proceedings of ION GNSS 21st International Technical Meeting of the Satellite Division, Savannah, US, pp 612-624

Ge M, Gendt G, Rothacher M, Shi C, Liu J (2008) Resolution of GPS carrier-phase ambiguities in precise point positioning (PPP) with daily observations. J Geod 82(7):389-399

Geng J (2009) Rapid re-convergence in real-time precise point positioning with ambiguity resolution. In: Proceedings of ION GNSS 22nd International Technical Meeting of the Satellite Division, Savannah, US, pp 2437-2448

Geng J, Teferle FN, Shi C, Meng X, Dodson AH, Liu J (2009) Ambiguity resolution in precise point positioning with hourly data. GPS Solut 13(4):263-270

Geng J, Teferle FN, Meng X, Dodson AH (2010) Towards PPP-RTK: Ambiguity resolution in real-time precise point positioning. Adv Space Res. doi:10.1016/j.asr.2010.03.030

Han S, Rizos C (2000) GPS multipath mitigation using FIR filters. Surv Rev 35(277):487-498

Hauschild A, Montenbruck O (2009) Kalman-filter-based GPS clock estimation for near real-time positioning. GPS Solut 13(3):173-182

Hernández-Pajares M, Juan JM, Sanz J, Colombo OL (2000) Application of ionospheric tomography to real-time GPS carrier-phase ambiguities resolution, at scales of 400-1000 km and with high geomagnetic activity. Geophys Res Lett 27(13):2009-2012

Kashani I, Wielgosz P, Grejner-Brzezinska D (2007) The impact of the ionospheric correction latency on long-baseline instantaneous kinematic GPS positioning. Surv Rev 39(305):238-251

Kim D, Serrano L, Langley R (2006) Phase wind-up analysis: Assessing real-time kinematic performance. GPS World 17(9):58-64

Kouba J (2009) A simplified yaw-attitude model for eclipsing GPS satellites. GPS Solut 13(1):1-12

Laurichesse D, Mercier F, Berthias JP, Broca P, Cerri L (2009) Integer ambiguity resolution on undifferenced GPS phase measurements and its application to PPP and satellite precise orbit determination. Navigation: Journal of the Institute of Navigation 56(2):135-149

Melbourne WG (1985) The case for ranging in GPS-based geodetic systems. In: Proceedings of First International Symposium on Precise Positioning with the Global Positioning System, US, pp 373-386

Senior KL, Ray JR, Beard RL (2008) Characterization of periodic variations in the GPS satellite clocks. GPS Solut 12(3):211-225

Shan S, Bevis M, Kendrick E, Mader GL, Raleigh D, Hudnut K, Sartori M, Phillips D (2007) Kinematic GPS solutions for aircraft trajectories: Identifying and minimizing systematic height errors associated with atmospheric propagation delays. Geophys Res Lett 34:L23S07

Shi C, Zhao Q, Geng J, Lou Y, Ge M, Liu J (2008) Recent development of PANDA software in GNSS data processing. In: Proceedings of the Society of Photographic Instrumentation Engineers, 7285:72851S

Stoew B, Nilsson T, Elgered G, Jarlemark POJ (2007) Temporal correlation of atmospheric mapping function errors in GPS estimation. J Geod 81(5):311-323

Teunissen PJG (1996) An analytical study of ambiguity decorrelation using dual frequency code and carrier phase. J Geod 70(8):515-528

Teunissen PJG (1997) On the sensitivity of the location, size and shape of the GPS ambiguity search space to certain changes in the stochastic model. J Geod 71(9):541-551

Teunissen PJG, de Jonge PJ, Tiberius CCJM (1997) The least-squares ambiguity decorrelation adjustment: its performance on short GPS baselines and short observation spans. J Geod 71(10):589-602

Wübbena G (1985) Software developments for geodetic positioning with GPS using TI-4100 code and carrier measurements. In: Proceedings of First International Symposium on Precise Positioning with the Global Positioning System, US, pp 403-412

Zumberge JF, Heflin MB, Jefferson DC, Watkins MM, Webb FH (1997) Precise point positioning for the efficient and robust analysis of GPS data from large networks. J Geophys Res 102(B3):5005-5017

Fig. 1 Distribution of 1-Hz test stations across Europe among which black solid squares denote stations used for real-time satellite clock determination

Fig. 2 RMS of the prediction errors of ionospheric delays under different time window widths which are labeled alongside the solid circles, different time latencies and different elevation angles: a) >30° and b) ≤ 30°

Fig. 3 Van trajectory consisting of four phases: 1) it stopped on the car park with an open sky view; 2) it moved along the red routes escorted by tall buildings, large trucks and thick trees; 3) it stopped again on the car park; 4) it moved along the blue routes on the car park with a few thick trees around. A reference station was located at IESSG. The upper inset shows the distances between six reference stations and IESSG, whereas the lower inset shows the satellite number and the time spans for the four phases. "LT" denotes local time

Fig. 4 Position differences from the ground truth for the East, North and Up components. From top to bottom show the ambiguity-float solutions, ambiguity-fixed solutions without and with rapid re-convergences (RRC), ambiguity-fixed solutions supported by a dense network (network PPP) and network RTK solutions. The symbol "√" denotes the time when ambiguity-fixed solutions are achieved, whereas "×" denotes the time when ambiguity-fixed solutions are totally lost

Table 1 Performance of rapid re-convergences within 5 s under different time latencies. A success rate is the ratio (*within parentheses*) between the number of rapid re-convergences (*before slashes*) and the total number of re-convergences (*behind slashes*). Time to fix is the real-valued mean time for all rapid re-convergences

Time latency	Wide-lane ambiguity resolution		Narrow-lane ambiguity resolution	
(s)	Success rate (%)	Time to fix (s)	Success rate (%)	Time to fix (s)
10	36459/36665 (99.4)	1.00	36159/36618 (98.7)	0.02
30	35236/35822 (98.4)	1.01	35223/35720 (98.6)	0.02
60	33782/34632 (97.5)	1.02	33860/34472 (98.2)	0.03
120	31003/32333 (95.9)	1.03	31011/32060 (96.7)	0.05
180	28060/30070 (93.3)	1.05	28024/29500 (95.0)	0.09
240	25134/28024 (89.7)	1.10	25058/27088 (92.5)	0.12
300	22417/26137 (85.8)	1.17	21875/24465 (89.4)	0.15

Figure 1

Click here to download high resolution image

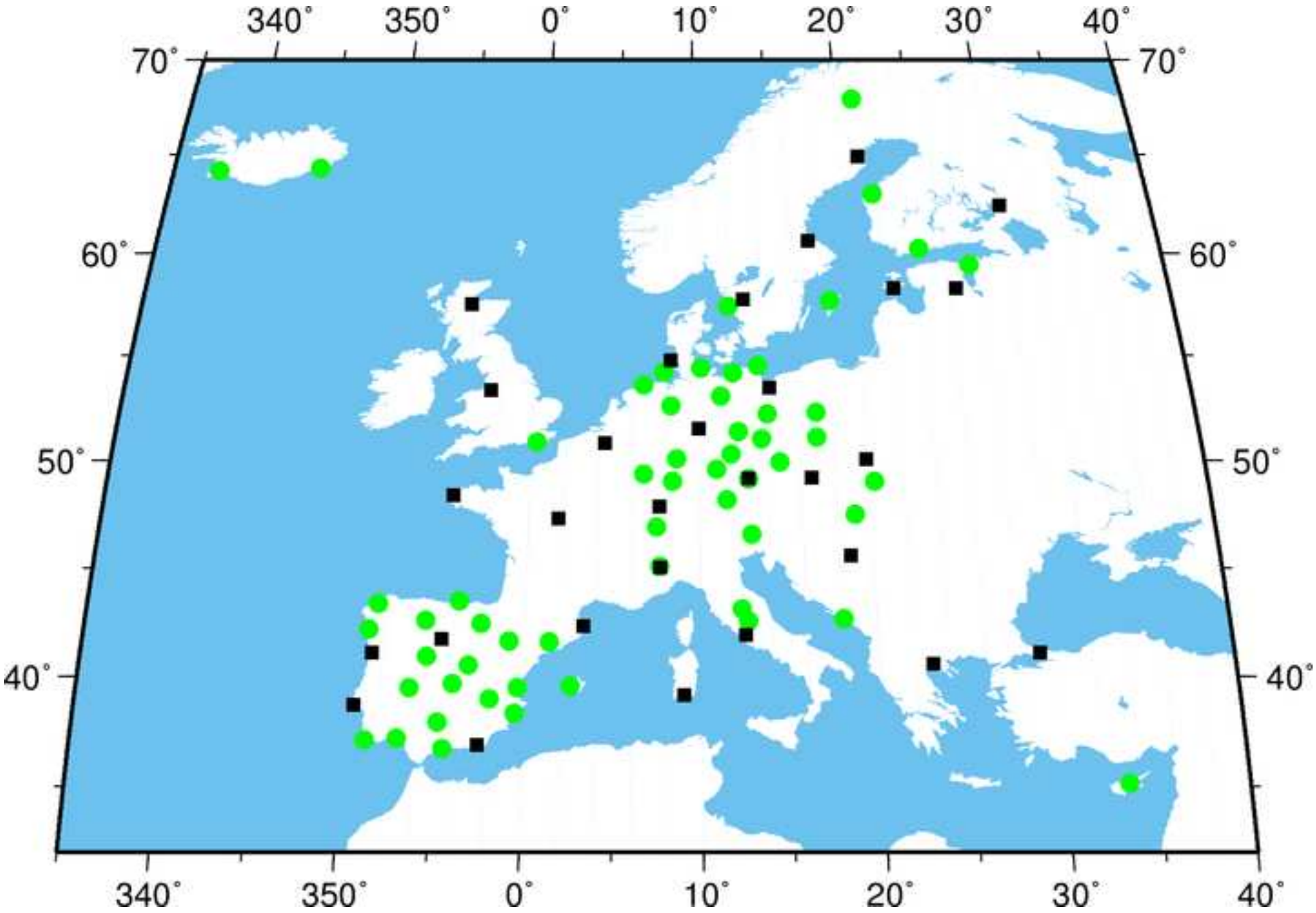

Figure 2

Click here to download high resolution image

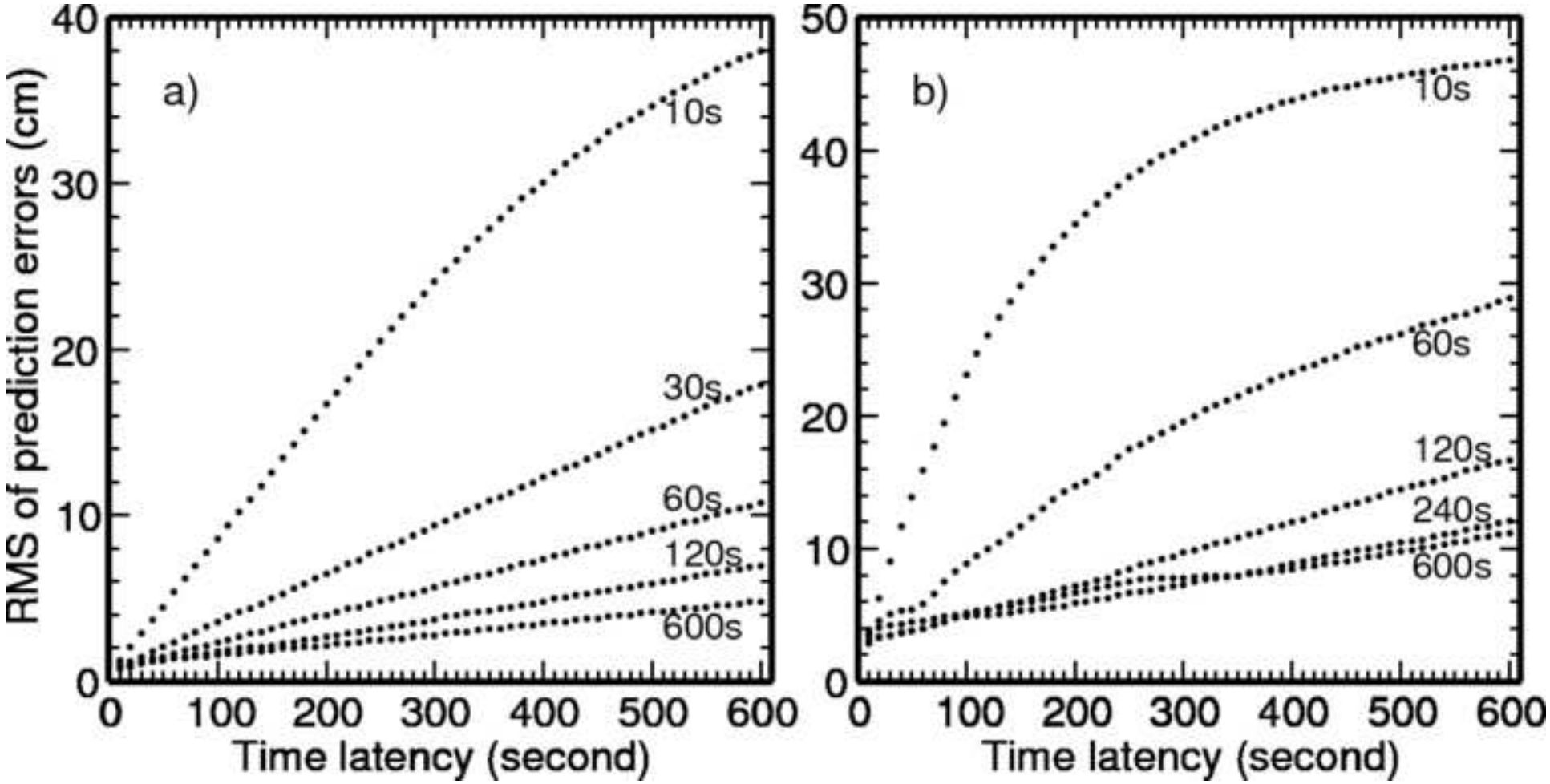

Figure 3

Click here to download high resolution image

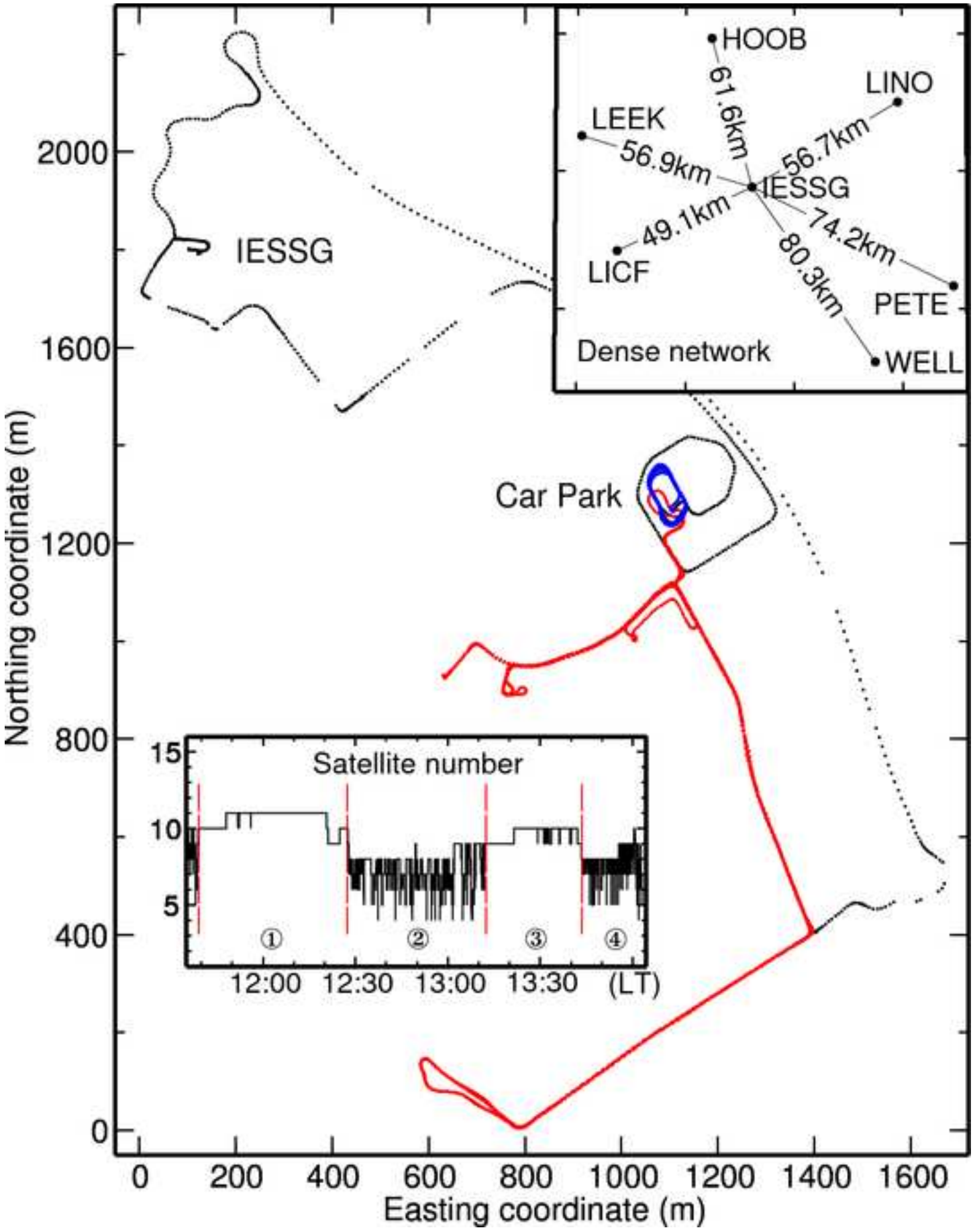

Figure 4

Click here to download high resolution image